From crystal steps to continuum laws: Behavior near large facets in one dimension

Dionisios Margetis [a,b,c,*], Kanna Nakamura [a]

[a] Department of Mathematics, University of Maryland, College Park, MD 20742, United States
[b] Institute for Physical Science and Technology, University of Maryland, College Park, MD 20742, United States
[c] Center for Scientific Computation and Mathematical Modeling, University of Maryland, College Park, MD 20742, United States

ABSTRACT

The passage from discrete schemes for surface line defects (steps) to nonlinear macroscopic laws for crystals is studied via formal asymptotics in one space dimension. Our goal is to illustrate by explicit computations the *emergence* from step motion laws of continuum-scale power series expansions for the slope near the edges of large, flat surface regions (facets). We consider surface diffusion kinetics via the Burton, Cabrera and Frank (BCF) model by which adsorbed atoms diffuse on terraces and attach–detach at steps. *Nearest-neighbor* step interactions are included. The setting is a monotone train of N steps separating two semi-infinite facets at fixed heights. We show *how* boundary conditions for the continuum slope and flux, and expansions in the height variable near facets, may emerge from the algebraic structure of discrete schemes as $N \to \infty$. Our technique relies on the use of self-similar discrete slopes, conversion of discrete schemes to sum equations, and their reduction to nonlinear integral equations for the continuum-scale slope. Approximate solutions to the continuum equations near facet edges are constructed formally by direct iterations. For elastic-dipole and multipole step interactions, the continuum slope is found in agreement with a previous hypothesis of 'local equilibrium'.

© 2011 Elsevier B.V. All rights reserved.

1. Introduction

The connection of many-particle schemes to nonlinear partial differential equations (PDEs) has been the subject of extensive studies in non-equilibrium statistical mechanics. This perspective has been explored in various physical contexts; for discussions see, e.g., [1,2].

In epitaxial phenomena, "particles" are interacting line defects (steps) of atomic size that move on crystal surfaces by mass conservation [3]. At the nanoscale, the motion of steps is described by large systems of differential equations for step positions. At the macroscale, this description is often reduced conveniently to nonlinear PDEs for macroscopic variables, e.g., for the surface height and slope profiles [4–11].

The PDEs are believed to be valid away from macroscopically flat surface regions known as "facets". Spohn [12] treated edges of facets as free boundaries, where in principle boundary conditions for the associated PDEs must be imposed. Such conditions are often formulated, explicitly or implicitly, within the continuum

framework [12–16] rather than derived directly from steps. The incorporation of facets into continuum evolution laws is a rich yet largely unexplored problem [17,7,18,19].

In this paper we address aspects of the question: what are the boundary conditions and near-facet expansions for continuum-scale variables *consistent* with step motion? We focus on two semi-infinite facets separated by a monotone train of N steps interacting entropically and as elastic dipoles in one space dimension (1D). This setting captures certain features of a finite crystal. From a continuum viewpoint our main results may not be overall surprising: in surface diffusion, the large-scale slope and flux vanish at facet edges. Our technique shows *what local behavior* (in space) of the slope *emerges* from the structure of discrete schemes for crystal steps. In order to simplify the analysis, we focus on documented *self-similar* solutions for the surface slope profile.

The same physical system is studied in [15] for *diffusion limited* (DL) kinetics via scaling arguments and numerics for step equations as well as for the PDE describing the slope profile. In this work, a self-similarity *ansatz* is used and verified numerically by discrete schemes. However, in [15] the continuum surface slope and flux are *assumed* to vanish at facet edges, with the slope behaving as $\mathcal{O}(\bar{x}^{1/2})$ for small distance $\bar{x}$ from the facet. These speculations led to numerical continuum solutions in excellent agreement with step simulation data [15].

* Corresponding author at: Department of Mathematics, University of Maryland, College Park, MD 20742, United States. Tel.: +1 301 405 5455; fax: +1 301 314 0827.
 E-mail addresses: dio@math.umd.edu (D. Margetis), nakamura@math.umd.edu (K. Nakamura).

Here, motivated by the analysis by Al Hajj Shehadeh et al. [19], we aim to shed some light on the studies in [15] by adopting a two-scale perspective. First, we use self-similar solutions for finite N to connect the discrete schemes to a continuum description for the slope as a function of height away from facets. The discrete schemes are converted to sum equations, which approach integral equations (see Propositions 1 and 2 of Section 3); the latter reveal power series expansions in the height variable. Second, we propose extensions such as *multipole* nearest-neighbor step interactions and special kinetics of extremal steps. We address surface diffusion in the absence of external material deposition. In fact, the evaporation–condensation case is exactly solvable under (assumed) self-similarity and will be invoked for comparison purposes.

1.1. Microscale: Burton–Cabrera–Frank (BCF) model

It is of interest to review elements of epitaxy for crystals; for extensive reviews see, e.g., [20–23]. The morphological evolution of crystal surfaces is driven by the motion of atomic steps separating nanoscale terraces, as was first predicted by Burton, Cabrera and Frank ("BCF") [24]. Three basic ingredients of the BCF model for surface diffusion are: (i) motion of steps by mass conservation; (ii) diffusion of adsorbed atoms ("adatoms") on terraces; and (iii) attachment and detachment of atoms at steps.

Another transport process is evaporation–condensation: atoms are exchanged between step edges and the surrounding vapor. We neglect atom desorption on terraces and diffusion along step edges [3], and leave out material deposition from the above. Hence, the surface is expected to relax by lowering its energy. Furthermore, we consider entropic and elastic-dipole *nearest-neighbor* step interactions [3,25,26]; see Section 4.1 for an extension.

1.2. Macroscopic limit and previous works

The BCF framework is our starting point. In the macroscopic limit the step size approaches zero while the step density is kept fixed. Our analysis is formal, i.e., it invokes simplifying assumptions which may be provable and avoids rigor. For instance, starting with a monotone step train (at $t = 0$), we assume that the discrete slopes, $m_j(t)$ (j: step number, t: time), and continuum-scale slope, $m(h, t)$ (h: height), are positive on the sloping surface for $t > 0$ and the continuum limit makes sense. We posit self-similarity for finite N; presumably, this is reached for long enough times [15,19] in various kinetic regimes, but this property is not proved here. In the same vein, the persistence of semi-infinite facets during evolution is hypothesized.

This formal approach enables us to explore modifications of the energetics and kinetics of the step model. Our arguments indicate how microscale mechanisms of step kinetics can possibly control the slope behavior at the macroscale.

Our work has been inspired by [19], where the relaxation of the same step configuration is studied rigorously via the l^2-steepest descent of a discrete energy functional under *attachment–detachment limited* (ADL) kinetics. In this case, the dominant process is the exchange of atoms at step edges. Notably, [19] invokes ordinary differential equations (ODEs) for *discrete slopes* at the nanoscale, and a PDE for the surface slope as a function of height at the macroscale. In [19], the positivity of discrete slopes and convergence of the discrete self-similar solution to a continuum self-similar one with zero slope at facet edges are proved; the condition of zero flux emerges as a "natural boundary condition" from the steepest descent. An analogous method for DL kinetics appears to be elusive at the moment.

Israeli et al. [27] study self-similar slope profiles under evaporation–condensation and surface diffusion with ADL kinetics for three 1D step geometries. Their step trains are semi-infinite, and thus differ from the *finite* step train studied here and in [19]; hence, direct comparisons to results of [27] are not compelling. By contrast to our setting, the self-similar slopes in [19] do not decay with time. In [27], the condition of zero slope at the facet edge and a power series expansion for the slope are imposed at the outset.

We adopt the use of the height as an independent variable [6, 19], which is a convenient Lagrangian coordinate of motion [28,15]. An advantage of this choice in the present setting, where facets are at fixed heights, is the elimination of free boundaries, as pointed out in [19]. We invoke equations for the discrete slopes in surface diffusion, following [7,29,19].

1.3. Goals and paper organization

Our intention with the present work is twofold. First, we aim to illustrate explicitly how boundary conditions for the continuum-scale slope and flux, and power series expansions in the space coordinate for the slope, are plausibly related to the algebraic structure of the discrete laws. In surface diffusion, these laws consist of three schemes: (i) the step velocity in terms of flux; (ii) the flux in terms of step chemical potential (a thermodynamic force); and (iii) the step chemical potential in terms of the discrete slope cubed for elastic-dipole step interactions. Our method addresses both DL and ADL kinetics.

Our second goal is to test the hypothesis of "local equilibrium" applied for facet edges within the continuum [15,14]. By this hypothesis, the surface slope vanishes as the square root of the distance from edges of zero-slope facets, if steps interact as elastic dipoles. This behavior is speculated by analogy with equilibrium crystal shapes on the basis of a surface free energy density proportional to the slope cubed [30–32].

The remainder of the paper is organized as follows. In Section 2, we formulate ODEs for discrete slopes. In Section 3, we study the emergence from discrete schemes of continuum-scale expansions for the slope near facets through iterations of integral equations. In Section 4, we discuss possible extensions. Section 5 summarizes our results. The appendices provide technical derivations and a study of the evaporation–condensation case invoked in the main text.

Units. We use nondimensional quantities via scaling of coordinates and other variables. The atomic area, terrace diffusivity, Boltzmann energy ($k_B T$) and step–step interaction strength are set equal to unity, since the respective dimensional parameters can be consolidated into a time scale.

2. Formulation of step motion laws

The step geometry is shown in Fig. 1. The system consists of $N + 1$ steps at positions $x = x_j(t)$, where $j = 0, \ldots, N$ and $t \geq 0$. The steps have constant size a, and separate two semi-infinite plateaus at fixed heights, $h = 0$ for $x < x_0(t)$ and $h = H \gg a$ for $x > x_N(t)$; cf. [15,19].

Set $\tilde{x} = x/H$ and $\tilde{h} = h/H$ and drop the tildes; thus, $(N + 1)\epsilon = 1$ (where $N \gg 1$ and $\epsilon \ll 1$), $0 \leqslant h \leqslant 1$ and a is replaced by $\epsilon = a/H$. Following [19], we employ the discrete slopes, m_j, as dependent variables:

$$m_j(t) := \frac{\epsilon}{x_{j+1}(t) - x_j(t)}, \quad j = 0, 1, \ldots, N - 1. \tag{1}$$

We *assume* that m_j are positive for all $t > 0$, given that $m_j > 0$ at $t = 0$.
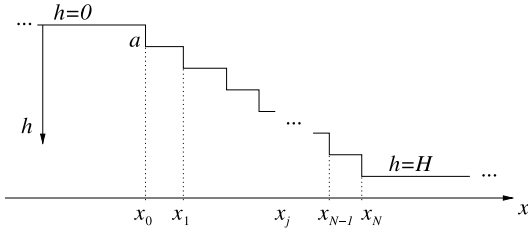
Fig. 1. Geometry in 1D (cross section): the step height is a; the step position is x_j; and the semi-infinite facets are located at heights $h = 0$ (top) and $h = H$ (bottom).

Next, we describe thermodynamic elements of step motion. For entropic and elastic-dipole step interactions, the energy of the step train is [3,25,26]

$$E_N = \frac{1}{2} \sum_{i=0}^{N-1} \left(\frac{\epsilon}{x_{i+1} - x_i} \right)^2 = \frac{1}{2} \sum_{i=0}^{N-1} m_i^2. \tag{2}$$

The chemical potential of the jth step is [3]

$$\mu_j = \frac{\delta E_N}{\delta x_j} = \epsilon^{-1} \left[\left(\frac{\epsilon}{x_{j+1} - x_j} \right)^3 - \left(\frac{\epsilon}{x_j - x_{j-1}} \right)^3 \right]$$

$$= \epsilon^{-1}(m_j^3 - m_{j-1}^3), \tag{3a}$$

where $j = 1, \ldots, N - 1$; for the *extremal* steps at $x = x_0, x_N$ we have

$$\mu_0 = \epsilon^{-1} m_0^3, \qquad \mu_N = -\epsilon^{-1} m_{N-1}^3. \tag{3b}$$

In surface diffusion, the step velocity, v_j, is driven by the adatom fluxes across step edges. By contrast, in evaporation–condensation v_j is driven by the step chemical potential [3,12]; see Appendix A.

2.1. Surface diffusion process

The step velocity law is

$$v_j = \frac{dx_j}{dt} = \dot{x}_j = \epsilon^{-1}[\varphi_{j-1}(x_j) - \varphi_j(x_j)], \quad j = 1, \ldots, N - 1; \tag{4}$$

$\varphi_j(x) = -\partial_x \rho_j(x)$ is the adatom flux on the jth terrace ($x_j < x < x_{j+1}$), (where the diffusivity is set to unity). The adatom density $\rho_j(x)$ obeys $\partial_x^2 \rho_j = \partial_t \rho_j \approx 0$ in the quasisteady regime [3]. By linear kinetics, we have [3]

$$-\varphi_j = 2\kappa (\rho_j - \rho_j^{eq})|_{x_j}, \qquad \varphi_j = 2\kappa (\rho_j - \rho_{j+1}^{eq})|_{x_{j+1}}, \tag{5}$$

where 2κ is a kinetic rate for the exchange of atoms at a step edge, the factor of 2 is included for later algebraic convenience, and $\rho_j^{eq} \approx 1 + \mu_j$ is an equilibrium density [3]. By enforcement of (5), we compute $\rho_j(x)$ and, thus, $\phi_j(x)$:

$$\varphi_j(x) = -\frac{\kappa}{1 + \kappa (x_{j+1} - x_j)} (\mu_{j+1} - \mu_j), \quad j = 0, \ldots, N - 1. \tag{6a}$$

Eq. (4) needs to be extended to $j = 0, N$. By taking into account $\rho_j(x)$ for $j = -1, x < x_0$ and $j = N, x > x_N$, we find the plateau fluxes

$$\varphi_{-1}(x) = 0 \quad x < x_0, \qquad \varphi_N(x) = 0 \quad x > x_N. \tag{6b}$$

By combining (4) and (6) with (3), we obtain a system of ODEs for m_j [15,33]. These equations are simplified in the following two regimes.

ADL kinetics: $m_j \gg \kappa\epsilon$. The equations of motion are reduced to [19]

$$\frac{\dot{m}_j}{m_j^2} = -\epsilon^{-4}(m_{j+2}^3 - 4m_{j+1}^3 + 6m_j^3 - 4m_{j-1}^3 + m_{j-2}^3), \tag{7a}$$

for $j = 0, \ldots, N - 1$, along with the conditions

$$m_{-1} = 0 = m_N,$$

$$m_0^3 - 2m_{-1}^3 + m_{-2}^3 = 0 = m_{N-1}^3 - 2m_N^3 + m_{N+1}^3. \tag{7b}$$

In (7a), we appropriately rescaled time (or set $\kappa\epsilon = 1$).

We apply the ansatz $m_j(t) = P(t)M_j$, and find $P(t) = (Ct + K)^{-1/4}$; set $C = 4$. In [19], the existence and uniqueness of this discrete similarity solution is shown by proving the existence of a unique positive critical point of a discrete energy. Further, in [19] the discrete slope evolution is recast to an l^2-steepest descent with respect to this energy; any solution of the ODE system for m_j with a positive definite initial condition approaches the similarity solution as $t \to \infty$. Numerical evidence is given in [19]. The M_j obey the *fourth-order* scheme

$$M_{j+2}^3 - 4M_{j+1}^3 + 6M_j^3 - 4M_{j-1}^3 + M_{j-2}^3$$

$$= \frac{\epsilon^4}{M_j}, \quad j = 0, \ldots, N - 1, \tag{8a}$$

$$M_{-1} = 0 = M_N,$$

$$M_0^3 - 2M_{-1}^3 + M_{-2}^3 = 0 = M_{N-1}^3 - 2M_N^3 + M_{N+1}^3. \tag{8b}$$

DL kinetics: $\kappa\epsilon \gg m_j$ [15]. The step equations reduce to the ODEs

$$\frac{\dot{m}_j}{m_j^2} = -\epsilon^{-4}[m_{j+1}(m_{j+2}^3 - 2m_{j+1}^3 + m_j^3)$$

$$- 2m_j(m_{j+1}^3 - 2m_j^3 + m_{j-1}^3)$$

$$+ m_{j-1}(m_j^3 - 2m_{j-1}^3 + m_{j-2}^3)], \quad j = 0, \ldots, N - 1; \tag{9a}$$

$$m_{-1} = 0 = m_N, \qquad m_{-2}, m_{N+1} : \text{finite}; \tag{9b}$$

thus, $m_{-1}(m_0^3 - 2m_{-1}^3 + m_{-2}^3) = 0 = m_N(m_{N-1}^3 - 2m_N^3 + m_{N+1}^3)$.

Now suppose $m_j(t) = P(t)M_j$. By (9) we have $\dot{p}/p^6 = -C < 0$ and find $P(t) = (5Ct + K)^{-1/5}$; set $C = 1$. The ensuing difference equation for M_j is

$$M_{j+1}(M_{j+2}^3 - 2M_{j+1}^3 + M_j^3) - 2M_j(M_{j+1}^3 - 2M_j^3 + M_{j-1}^3)$$

$$+ M_{j-1}(M_j^3 - 2M_{j-1}^3 + M_{j-2}^3) = \frac{\epsilon^4}{M_j}, \quad j = 0, \ldots, N - 1, \tag{10a}$$

with $M_j > 0$ and termination conditions

$$M_{-1} = 0 = M_N \quad \text{and} \quad M_{-2}, M_{N+1} : \text{finite}. \tag{10b}$$

3. Limits of discrete schemes and near-facet expansions

In this section we derive expansions for the continuum-scale slope near facets *directly* from schemes for discrete self-similar slopes in surface diffusion. We convert the discrete schemes to sum equations, and show that, as $\epsilon \downarrow 0$ with $h = (j + 1)\epsilon = \mathcal{O}(1)$ and $(N + 1)\epsilon = 1$, the sum equations become integral equations which indicate via iterations the slope behavior as $h \downarrow 0$ and $h \uparrow 1$. A mathematical addendum on the manipulation of difference schemes is given in Appendix B. The evaporation case is treated in Appendix C, where a continuum similarity solution is computed exactly in simple closed form.

In the limit $\epsilon \downarrow 0$, we assume that the discrete slopes, m_j, approach the surface slope in an appropriate weak sense [33]. In principle, given a sequence $\{u_j\}_{j=0}^{N-1}$ (e.g., $u = m$), we posit a continuous $u(h, t)$, $h \in (0, 1)$, such that for every (smooth) test function $\vartheta(h)$ with $\vartheta_j := \vartheta((j + 1)\epsilon)$ and $t > 0$,

$$\epsilon \sum_{j=0}^{N-1} \vartheta_j u_j(t) = (N + 1)^{-1} \sum_{j=0}^{N-1} \vartheta_j u_j(t) \xrightarrow[N \to \infty]{} \int_0^1 \vartheta(h) u(h, t) dh, \tag{11}$$

and write $u_j(\cdot) \rightharpoonup u(h, \cdot)$; assume convergence of these sums and integrals.

3.1. DL kinetics

We first focus on the self-similarity ansatz $m_j(t) = P(t)M_j = (5t+K)^{-1/5}M_j$ observed in [15], and set $\psi_j = M_j^3$. The fourth-order scheme (10) is split as

$$\psi_{j+1} - 2\psi_j + \psi_{j-1} = -\frac{\epsilon^2 \varphi_j}{\psi_j^{1/3}},$$

$$\varphi_{j+1} - 2\varphi_j + \varphi_{j-1} = -\frac{\epsilon^2}{\psi_j^{1/3}}; \tag{12a}$$

$$\psi_{-1} = 0 = \psi_N, \qquad \varphi_{-1} = 0 = \varphi_N; \quad j = 0, 1, \ldots, N-1. \tag{12b}$$

Recall that φ_j is the adatom flux on the jth terrace ($x_j < x < x_{j+1}$).

Proposition 1 (*A Continuum Limit in DL Kinetics*). *In the limit $\epsilon \downarrow 0$ with $m_j(t) \rightharpoonup P(t)m(h)$, discrete scheme (12) reduces to the integral equation*

$$\psi(h) = m(h)^3 = C_1 h - C_2 \int_0^h \frac{z(h-z)}{m(z)} dz$$
$$+ \int_0^h \int_0^z \frac{(h-z)(z-\zeta)}{m(z)m(\zeta)} d\zeta\, dz, \tag{13}$$

$0 < h < 1$; *thus,* $\lim_{h\downarrow 0} m(h) = 0 = \lim_{h\downarrow 0} \varphi(h)$ (φ: *flux*). *The constants C_1, C_2 are subject to respective conditions at $h = 1$: $\lim_{h\uparrow 1} m(h) = 0 = \lim_{h\uparrow 1} \varphi(h)$. By (13), a sufficiently differentiable $m(h)$ obeys $m[m(m^3)_{hh}]_{hh} = 1$.*

We abuse notation by using the symbol $m(h)$ for the h-dependent continuum similarity solution. The primary continuum variables are the slope, $m(h)$, and flux, $\varphi(h)$. Assume that the integrals in (13) converge and a solution exists appropriately.

Proof. We proceed along the lines of Appendix B.1; see formulas (B.1)–(B.4) in regard to expressing ψ_j in terms of the generating function (polynomial), $\Psi(s) = \sum_{j=0}^{N-1} \psi_j s^j$. Our strategy is to convert each of the second-order difference equations (12a) to a sum equation, treating their right-hand sides as forcing terms, f_j. The first one of (12a) leads to

$$\psi_j = (1+j)\psi_0 - \sum_{p=0}^{j-1}[(j+1)\epsilon - (p+1)\epsilon]\frac{\varphi_p}{\psi_p^{1/3}}\epsilon, \tag{14a}$$

after applying the first pair of conditions (12b); the coefficient ψ_0 is given by

$$(N+1)\psi_0 = \sum_{j=0}^{N-1}[(N+1)\epsilon - (j+1)\epsilon]\frac{\varphi_j}{\psi_j^{1/3}}\epsilon. \tag{14b}$$

The second one of equations (12a) with the last pair of conditions (12b) yields

$$\varphi_j = (1+j)\varphi_0 - \sum_{p=0}^{j-1}\frac{(j+1)\epsilon - (p+1)\epsilon}{\psi_p^{1/3}}\epsilon, \tag{15a}$$

where, by analogy with (14b),

$$(N+1)\varphi_0 = \sum_{j=0}^{N-1}[(N+1)\epsilon - (j+1)\epsilon]\psi_j^{-1/3}\epsilon. \tag{15b}$$

Now let $\epsilon \downarrow 0$ with $(N+1)\epsilon = 1$ and $(j+1)\epsilon = h = \mathcal{O}(1)$. By (14), we have

$$\psi_j \rightharpoonup \psi(h) = m(h)^3 = C_1 h$$
$$- \int_0^h (h-z)\frac{\varphi(z)}{m(z)} dz \quad 0 < h < 1; \tag{16a}$$

$$C_1 := \lim_{\epsilon\downarrow 0}(\epsilon^{-1}\psi_0) = \int_0^1 (1-z)\frac{\varphi(z)}{m(z)} dz. \tag{16b}$$

By (15), the analogous limit for φ_j is

$$\varphi_j \rightharpoonup \varphi(h) = C_2 h - \int_0^h \frac{h-z}{m(z)} dz \quad 0 < h < 1; \tag{17a}$$

$$C_2 := \lim_{\epsilon\downarrow 0}(\epsilon^{-1}\varphi_0) = \int_0^1 \frac{1-z}{m(z)} dz. \tag{17b}$$

By the definitions of C_1 and C_2, we infer $\lim_{h\uparrow 1} m(h) = 0 = \lim_{h\uparrow 1} \varphi(h)$. The combination of (16a) and (17a) recovers (13). Differentiations of the integral equations entail $m(m^3)_{hh} = -\varphi$, $m\varphi_{hh} = -1$, by which $m(m(m^3)_{hh})_{hh} = 1$. $\quad\square$

Corollary 1. *The constants C_1 and C_2 in (13) are positive. Further, for $0 < h < 1$, the flux $\varphi(h)$ is positive; thus, (a twice continuously differentiable) $m(h)^3$ is concave.*

The first statement in Corollary 1 follows from the definitions of C_1 and C_2 and the assumed positivity of the slope. Note that

$$C_1 = \int_0^1 \frac{1-z}{m(z)} \left[\int_0^z \frac{\zeta(1-z)}{m(\zeta)} d\zeta + \int_z^1 \frac{z(1-\zeta)}{m(\zeta)} d\zeta\right] dz.$$

The positivity of $\varphi(h) = -m(m^3)_{hh}$ follows from (17).

Near-facet expansion. In the spirit of Appendix C.2, notice that if $m(h) = \mathcal{O}(h^\alpha)$ as $h \downarrow 0$ for some $0 \leqslant \alpha < 1$, the integrals in (13) generate subdominant contributions of orders (from left to right) $\mathcal{O}(h^{3-\alpha})$ and $\mathcal{O}(h^{4-2\alpha})$. This observation motivates an iteration scheme for (13), or the system of (16a) and (17a). Successive local approximations of $m(h)$ as $h \downarrow 0$ are constructed via

$$m^{(n+1)}(h)^3 = C_1 h - \int_0^h (h-z)\frac{\varphi^{(n)}(z)}{m^{(n)}(z)} dz,$$

$$m^{(0)}(h) = (C_1 h)^{1/3};$$

$$\varphi^{(n+1)}(h) = C_2 h - \int_0^h \frac{h-z}{m^{(n)}(z)} dz, \qquad \varphi^{(0)}(h) = C_2 h, \tag{18}$$

where $m \sim m^{(n)}$, $\varphi \sim \varphi^{(n)}$ to $n+1$ terms; $n = 0, 1, \ldots$. The above construction produces a formal expansion of $m(h)$ in ascending powers of h. The first three terms are evaluated in Appendix D; the result reads

$$m(h) = (C_1 h)^{1/3} - \frac{3}{40}\frac{C_2}{C_1}h^2 + \frac{27}{700}C_1^{-4/3}h^{8/3} + \mathcal{O}(h^{11/3})$$
$$\text{as } h \downarrow 0. \tag{19}$$

Note the powers of h entering (19), i.e., 1/3 (leading order), 2 (first correction) and 8/3, in comparison to the powers 1/3, 1, 5/3 appearing in (C.13) of Appendix C for the evaporation–condensation case.

By the discrete scheme for $x_j(t)$, and $m_j(t) \sim M_j t^{-1/5}$, we find $x_j(t) \sim t^{1/5}X_j$ for large t; thus, $h = h(\eta)$ and $m(h(\eta)) = h'(\eta)$ where the similarity variable is $\eta = xt^{-1/5}$ [15]. By integration and inversion of (19), we find an expansion of $m(h(\eta))$ in the vicinity of the facet edge, as $\bar{\eta} = \eta - \eta_{f,L} \downarrow 0$, where $\eta_{f,L} = x_{f,L}(t)t^{-1/5}$ and $x_{f,L}(t)$ is the position of the left facet ($h = 0$):

$$m(h(\eta)) = \left(\frac{2}{3}\right)^{1/2} C_1^{1/2}\bar{\eta}^{1/2} - \frac{8}{315}C_2\bar{\eta}^3 + \frac{8}{945}\bar{\eta}^4 + \mathcal{O}(\bar{\eta}^{11/2}). \tag{20}$$

Note the absence of the powers 1, 3/2, 2, 5/2; cf. Eq. (A5) in [15]. Likewise, by mirror symmetry we can write the analogous expansion for $m(h)$ as $h \uparrow 1$.

Remark 1. Integral equation (13) can result from integrating the slope ODE $m[m(m^3)_{hh}]_{hh} = 1$ under the conditions $m \to 0$ and $\varphi \to 0$ as $h \downarrow 0$ and $h \uparrow 1$. Our technique exemplifies the passage to the continuum limit *via the integral equation* so that these conditions emerge directly from the difference scheme.

Remark 2. It is tempting to extend the results of Proposition 1 to the time-dependent setting (without self-similarity), where $m_j(t) \rightharpoonup m(h, t)$. The emergent pair of integral relations for $m(h, t)$ and the continuum flux, $\varphi(h, t)$, is

$$m(h, t)^3 = C_1(t)h - \int_0^h (h-z)\frac{\varphi(z, t)}{m(z, t)}\mathrm{d}z,$$

$$\varphi(h, t) = C_2(t)h - \int_0^h (h-z)\partial_t[m(z, t)^{-1}]\mathrm{d}z,$$
$$0 < h < 1,\ t > 0, \tag{21}$$

provided the integrals converge; $C_1(t)$ and $C_2(t)$ are subject to the vanishing of m and φ as $h \uparrow 1$. In principle, it may not be legitimate to iterate (21) in order to expand $m(h, t)$ near a facet edge, unless t is sufficiently large. By differentiation of (21), we obtain the PDE $\partial_t m = -m^2 \partial_h^2(m \partial_h^2 m^3)$ [14,15].

Remark 3. By (21), the slope is $m(h(x, t), t) = \mathcal{O}((x - x_f(t))^{1/2})$ as $x \to x_f(t)$ (position of the left or right facet edge) for sufficiently long times, consistent with the hypothesis of local equilibrium invoked in earlier continuum theories, e.g., in [14]. Further iterations are suggestive of the nature of the expansion for $m(h, t)$ in the vicinity of large facet edges. To compute coefficients of the expansion, it is algebraically convenient to make the substitution $m(h, t) = \sum_{n=1}^{\infty} A_n(t)(x - x_f(t))^{n/2}$ into the PDE for $m(h, t)$; then, the values $A_2 = A_3 = A_4 = A_5 = 0$ are recovered by dominant balance [15].

3.2. ADL kinetics

Next, we focus on fourth-order scheme (7), which is also the subject of [19]. By the similarity solution $m_j(t) = (4t + K)^{-1/4}M_j$, proved in [19], and $\psi_j = M_j^3$, the pertinent difference equations read

$$\psi_{j+2} - 4\psi_{j+1} + 6\psi_j - 4\psi_{j-1} + \psi_{j-2} = f_j = \epsilon^4 \psi_j^{-1/3}, \tag{22a}$$

for $j = 0, 1, \ldots, N - 1$, along with the conditions

$$\psi_{-1} = 0 = \psi_N,$$
$$\psi_0 - 2\psi_{-1} + \psi_{-2} = 0 = \psi_{N-1} - 2\psi_N + \psi_{N+1}; \tag{22b}$$

recall that $\varphi_j = -(\psi_{j+1} - 2\psi_j + \psi_{j-1})$ is the jth-terrace adatom flux. There are at least two routes to studying (22): either split it into two second-order schemes by using φ_j as an auxiliary variable, or leave the fourth-order scheme intact and use only ψ_j. We choose the latter route here.

Proposition 2 (*A Continuum Limit in ADL Kinetics*)**.** *In the limit $\epsilon \downarrow 0$, discrete scheme (22) reduces to the integral equation*

$$\psi(h) = m(h)^3 = C_1 h - C_3 h^3 + \frac{1}{6}\int_0^h \frac{(h-z)^3}{m(z)}\mathrm{d}z,$$
$$0 < h < 1; \tag{23}$$

thus, $\lim_{h\downarrow 0} m(h) = 0 = \lim_{h\downarrow 0}\varphi(h)$ *(φ: flux). The constants C_1 and C_3 are subject to respective conditions at $h = 1$: $\lim_{h\uparrow 1} m(h) = 0 = \lim_{h\uparrow 1}\varphi(h)$. By (23), (a sufficiently differentiable) $m(h)$ satisfies $m(m^3)_{hhhh} = 1$; cf. [19].*

By our usual practice, we assume that the integral in (23) converges and a solution of the integral equation exists in some appropriate sense.

Proof. We treat the f_j of (22a) as given forcing terms and solve for ψ_j with recourse to the generating polynomial, $\Psi(s)$; see Appendix B.2 for details. After some algebra, the variables ψ_j are found to be

$$\psi_j = \frac{1}{6}\Bigg[(\psi_1 - 2\psi_0)j^2(j + 3) + 2(\psi_0 + \psi_1)j + 6\psi_0$$
$$+ \epsilon^4 \sum_{p=0}^{j-2}(j - p - 1)(j - p)(j - p + 1)\psi_p^{-1/3}\Bigg],$$
$$j = 0, \ldots, N - 1, \tag{24}$$

where

$$\psi_1 - 2\psi_0 = \frac{-NF(1) + F'(1)}{N + 1}, \tag{25a}$$

$$2(N + 1)(\psi_1 + \psi_0) = N(2N - 1)F(1) + (2N^2 - 5N + 2)F'(1) - 3(N - 1)F''(1) + F'''(1), \tag{25b}$$

$$\psi_0 = \frac{N(2N + 1)F(1) + N(2N - 5)F'(1) - 3(N - 1)F''(1) + F'''(1)}{6(N + 1)}. \tag{25c}$$

Recall $F(s) = \sum_{j=0}^{N-1} f_j s^j$. The prime in (25) denotes the derivative in s.

Now let $N \to \infty$, and $\epsilon \downarrow 0$ with $(N + 1)\epsilon = 1$. By formulas (25), we find

$$\frac{\psi_1 - 2\psi_0}{\epsilon^3} \xrightarrow[\epsilon\downarrow 0]{} -\int_0^1 \frac{1-z}{m(z)}\mathrm{d}z, \tag{26a}$$

$$\frac{\psi_0 + \psi_1}{\epsilon} \xrightarrow[\epsilon\downarrow 0]{} \frac{1}{2}\int_0^1 \frac{1 - z - (1-z)^3}{m(z)}\mathrm{d}z, \tag{26b}$$

$$\psi_0 = \mathcal{O}(\epsilon) \to 0. \tag{26c}$$

For fixed height $h = (j + 1)\epsilon$ (with $j \to \infty$), we let $\psi_j \rightharpoonup \psi(h)$, thus reducing sum equation (24) to integral equation (23) with

$$C_1 := \lim_{\epsilon\downarrow 0}\frac{\psi_0 + \psi_1}{3\epsilon} = \frac{1}{6}\int_0^1 \frac{1 - z - (1-z)^3}{m(z)}\mathrm{d}z, \tag{27a}$$

$$C_3 := -\lim_{\epsilon\downarrow 0}\frac{\psi_1 - 2\psi_0}{6\epsilon^3} = \frac{1}{6}\int_0^1 \frac{1-z}{m(z)}\mathrm{d}z, \tag{27b}$$

and the neglect of ψ_0. The resulting continuum-scale slope $m(h)$ vanishes as $h \downarrow 0$. In addition, $\varphi_j \rightharpoonup \varphi(h)$ with $\lim_{h\downarrow 0}\varphi(h) = 0$, as verified by (23). Eq. (27) imply that the slope and flux also vanish as $h \uparrow 1$. The differentiation of (23) furnishes the ODE $m(m^3)_{hhhh} = 1$, where $\varphi(h) = -(m^3)_{hh}$. □

Corollary 2. *The constants C_1 and C_3 entering (23) are positive. Further, the large-scale flux, $\varphi(h) = -(m^3)_{hh}$, is positive for $0 < h < 1$.*

Corollary 2 declares the concavity of $\psi(h) = m(h)^3$ proved in [19].

Near-facet expansion. In the spirit of Appendix C.2 and Section 3.1, a formal expansion for the slope near facet edges can plausibly be derived by iterations of (23). The ensuing slope behavior is $m(h) = (C_1 h)^{1/3} + \mathcal{O}(h^{7/3})$ as $h \downarrow 0$. The leading-order term is compatible with local equilibrium. Hence, with $\eta = xt^{-1/4}$, we have (cf. (20))

$$m(h(\eta)) = \left(\frac{2}{3}\right)^{1/2} C_1^{1/2}\bar{\eta}^{1/2} + \mathcal{O}(\bar{\eta}^{7/2}) \quad \text{as } \bar{\eta} \to 0;$$
$$\bar{\eta} = t^{-1/4}(x - x_f(t)). \tag{28}$$

Remark 4. The derivation can be extended to the full time dependent setting, where $m_j(t) \rightharpoonup m(h, t)$. The integral relation consistent with step laws is

$$m(h, t)^3 = C_1(t)h - C_3(t)h^3$$

$$+ \frac{1}{6} \int_0^h (h - z)^3 \partial_t [m(z, t)^{-1}] dz, \qquad (29)$$

where $0 < h < 1$ and $t > 0$. The PDE reads $\partial_t m = -m^2 \partial_h^4 m^3$ [19].

4. Extensions

In this section we discuss two possible extensions of our formulation. First, we address different laws of nearest-neighbor step interactions; in this case, the slope behavior at facet edges, i.e., the exponent $1/2$ in the leading-order terms of (20) and (28), is modified accordingly. Second, we propose a *toy model* where the kinetics of attachment–detachment at extremal steps is different from other steps. Our discussion aims to indicate the role that individual steps may play in the derivation of boundary conditions in the continuum setting.

Another plausible extension concerns the presence of an Ehrlich-Schwoebel barrier, by which the attachment–detachment law for all steps is characterized by different kinetic rates, say κ_u and κ_d, for up- and down-steps [34,35]. In this case, the effective kinetic rate for the adatom flux is the harmonic average of κ_u and κ_d [11]. Hence, our analysis remains essentially intact.

4.1. Multipole nearest-neighbor step interactions

Next, we discuss continuum-scale implications of the step energy [11]

$$E_N(\{x_j\}_{j=0}^N) = \frac{1}{\alpha} \sum_{i=0}^{N-1} \left(\frac{\epsilon}{x_{i+1} - x_i} \right)^\alpha = \frac{1}{\alpha} \sum_{i=0}^{N-1} m_i^\alpha \quad \alpha > 1, \qquad (30)$$

which in principle includes step multipole interactions for integer $\alpha \geqslant 2$ [26]; $\alpha = 2$ for dipole step interactions. The jth-step chemical potential is

$$\mu_j = \frac{\delta E_N}{\delta x_j} = \epsilon^{-1}(m_j^{\alpha+1} - m_{j-1}^{\alpha+1}), \quad j = 1, \ldots, N-1; \qquad (31)$$

in addition, $\mu_0 = \epsilon^{-1} m_0^{\alpha+1}$ and $\mu_N = -\epsilon^{-1} m_{N-1}^{\alpha+1}$. Formulas for the adatom flux and step velocity ensue from Section 2 via $m_j^3 \Rightarrow m_j^{\alpha+1}$ in μ_j.

For instance, in DL kinetics the discrete scheme for steps now reads

$$\frac{\dot{m}_j}{m_j^2} = -\epsilon^{-4}[m_{j+1}(m_{j+2}^{\alpha+1} - 2m_{j+1}^{\alpha+1} + m_j^{\alpha+1})$$

$$- 2m_j(m_{j+1}^{\alpha+1} - 2m_j^{\alpha+1} + m_{j-1}^{\alpha+1})$$

$$+ m_{j-1}(m_j^{\alpha+1} - 2m_{j-1}^{\alpha+1} + m_{j-2}^{\alpha+1})],$$

$$j = 0, \ldots, N-1; \qquad (32a)$$

$$m_{-1} = 0 = m_N, \qquad m_{-2}, m_{N+1} : \text{finite}. \qquad (32b)$$

Thus, the discrete self-similar slopes read $m_j(t) = [(\alpha + 3)t + K]^{-\frac{1}{\alpha+3}} M_j$.

To proceed along the lines of Section 3, let $\psi_j = M_j^{\alpha+1}$; or, more generally, $\psi_j(t) = m_j(t)^{\alpha+1}$. Our manipulations for ψ_j remain intact. The analogue of Proposition 1 contains the relation (cf. (13))

$$m(h)^{\alpha+1} = C_1 h - C_2 \int_0^h \frac{z(h-z)}{m(z)} dz$$

$$+ \int_0^h \int_0^z \frac{(h-z)(z-\zeta)}{m(z)m(\zeta)} d\zeta\, dz, \qquad (33)$$

where C_1 and C_2 are subject to the vanishing of slope and flux at $h = 1$.

Iterations of (33) yield a formal expansion of the slope near the facet edges. We obtain $m(h(x, t), t) = \mathcal{O}((x - x_f(t))^{1/\alpha})$ as $x \to x_f(t)$, the position of a facet edge, for sufficiently long times. This behavior manifests the intimate connection of step interaction law and near-facet expansion at equilibrium [30].

4.2. Special kinetics of extremal steps

In this section we explore the following scenario. Suppose the attachment–detachment law for extremal steps ($j = 0, N$) involves kinetic rates, say κ_L for $j = 0$ and κ_R for $j = N$, which may be different from κ. By linear kinetics, the fluxes impinging on these steps are taken to be

$$-\varphi_0 = 2\kappa_L(\rho_0 - \rho_0^{eq}) \quad x = x_0;$$
$$\varphi_{N-1} = 2\kappa_R(\rho_{N-1} - \rho_N^{eq}) \quad x = x_N. \qquad (34)$$

At the other steps, the kinetic rates remain 2κ. We study whether κ_L or κ_R can possibly distort nontrivially the previous boundary conditions in the macroscopic limit, *assuming this limit is well defined*. The 0th terrace adatom flux is $\varphi_0 = -\epsilon^{-1}(\bar{\kappa}\epsilon)m_0(\rho_1^{eq} - \rho_0^{eq})/(\bar{\kappa}\epsilon + m_0)$, where $\bar{\kappa} = 2(\kappa^{-1} + \kappa_L^{-1})^{-1}$. Without loss of generality, set $\kappa_R = \kappa \neq \kappa_L$ and define $\beta = \bar{\kappa}/\kappa > 0$. Hence, we restrict attention to the left facet edge ($h = 0$). It is tempting to claim that, in the limit $\epsilon \downarrow 0$, the detail of (34) *disappears*; and hence we recover a continuum-scale boundary condition of zero slope and flux. We discuss formally why this claim is consistent with steps if $\beta = \mathcal{O}(1)$. The situation is subtler if $\beta \leq \mathcal{O}(\epsilon^3)$.

We focus on ADL kinetics, where surface processes are limited by atom attachment–detachment at steps, and scale time by $\kappa\epsilon$. The motion laws for the discrete slopes are described by (7a) along with the *modified* termination conditions

$$m_{-1}^3 + (1 - \beta)(m_1^3 - 2m_0^3) = 0 = m_N^3, \qquad (35a)$$

$$m_0^3 - 2m_{-1}^3 + m_{-2}^3 = 0 = m_{N-1}^3 - 2m_N^3 + m_{N+1}^3. \qquad (35b)$$

Eq. (35b) states that the auxiliary discrete fluxes vanish, in accord with (7b); hence, we expect that the boundary conditions for the continuum-scale flux are intact. By contrast, (35a) indicates a nonzero m_{-1}, which in turn suggests the possibility of a nonzero continuum-scale slope as $h \downarrow 0$. (In view of (35a), the mirror symmetry of the system is removed.)

We proceed to convert (7a) to sum equations via the generating polynomial, $\Psi(s)$; see Appendix B.2. Let $\psi_j = m_j^3$. After some algebra, we find (cf. (24))

$$\psi_j = \frac{1}{6} \Big\{ \beta(\psi_1 - 2\psi_0)j^2(j + 3) + 2[\psi_0 + \psi_1$$

$$- 2(\beta - 1)(\psi_1 - 2\psi_0)]j + 6\psi_0 + \epsilon^4 \sum_{p=0}^{j-2} (j - p - 1)$$

$$\times (j - p)(j - p + 1)(d/dt)\psi_j(t)^{-1/3} \Big\}, \qquad (36)$$

where, with $F(s) = \epsilon^4 \sum_{j=0}^{N-1} s^j (\mathrm{d}/\mathrm{d}t) \psi_j(t)^{-1/3}$, the requisite coefficients are

$$\beta(\psi_1 - 2\psi_0) = \frac{-NF(1) + F'(1)}{N+1},$$

$$2(N+1)[\psi_0 + \psi_1 - 2(\beta - 1)(\psi_1 - 2\psi_0)]$$
$$= \left(2N^2 - N + 6\frac{\beta - 1}{\beta}\frac{N}{N+1}\right)F(1)$$
$$\quad + \left(2N^2 - 5N + 2 - 6\frac{\beta - 1}{\beta}\frac{1}{N+1}\right)F'(1)$$
$$\quad - 3(N-1)F''(1) + F'''(1),$$

$$6(N+1)\psi_0 = \left(2N^2 + N - 6N\frac{\beta - 1}{\beta}\frac{N}{N+1}\right)F(1)$$
$$\quad + \left(2N^2 - 5N + 6\frac{\beta - 1}{\beta}\frac{N}{N+1}\right)F'(1)$$
$$\quad - 3(N-1)F''(1) + F'''(1).$$

Note the term ψ_0 entering the right-hand side of (36). The question arises as to whether $\psi_0 = \mathcal{O}(1)$ as $\epsilon \downarrow 0$ by manipulation of the parameter β.

Consider the limit of (36) as $N \to \infty$ with $\epsilon(N + 1) = 1$. By Section 3.2, we infer that any contribution of β is negligible if $\beta = \mathcal{O}(1)$; the macroscopic laws are identical to those for $\beta = 1$ (Section 3.2): the slope *and* flux vanish at the facet edges. These conditions appear to persist provided $\beta > \mathcal{O}(N^{-3})$.

Now suppose $\beta = \breve{\beta}/N^3$, $\breve{\beta} = \mathcal{O}(1) > 0$, while the continuum limit makes sense, e.g., $N^{4-n} F'^{(n)}(1) \to \int_0^1 z^{n-1} \partial_t [m(z,t)^{-1}]\mathrm{d}z = \mathcal{O}(1)$ as $N \to \infty$; $n = 1, 2, 3, 4$ and $F'^{(n)}(s)$ denotes the nth-order derivative of $F(s)$. We find

$$m(h,t)^3 = C_0(t) + C_1(t)h - C_3(t)h^3$$
$$\quad + \frac{1}{6}\int_0^h (h-z)^3 \partial_t[m(z,t)^{-1}]\mathrm{d}z; \tag{37}$$

cf. (29). The coefficients $C_0(t)$, $C_1(t)$ and $C_3(t)$ are found to be

$$C_0(t) = \lim_{\epsilon \downarrow 0} \psi_0(t) = \breve{\beta}^{-1}\int_0^1 (1-z)\partial_t[m(z,t)^{-1}]\mathrm{d}z,$$

which signifies the nonzero value of the continuum slope as $h \downarrow 0$, and

$$C_1(t) = \lim_{\epsilon \downarrow 0} \frac{\psi_1(t) + \psi_0(t) - 2(\beta-1)[\psi_1(t) - 2\psi_0(t)]}{3\epsilon}$$
$$= \frac{1}{6}\int_0^1 [(1 - 6\breve{\beta}^{-1})(1-z) - (1-z)^3]\partial_t[m(z,t)^{-1}]\mathrm{d}z,$$

$$C_3(t) = -\lim_{\epsilon \downarrow 0} \frac{\beta[\psi_1(t) - 2\psi_0(t)]}{6\epsilon^3}$$
$$= \frac{1}{6}\int_0^1 (1-z)\partial_t[m(z,t)^{-1}]\mathrm{d}z.$$

Note that if $\breve{\beta} \gg 1$, (37) reduces to the macroscopic limit of Section 3.2.

A sufficiently small β forces the microscale flux at the top step to become small; thus, the motion of the extremal step tends to be 'frozen' and the density of steps increases in the vicinity of the left facet edge. Interestingly, our heuristic analysis indicates the critical scaling $\beta = \mathcal{O}(N^{-3})$ for this 'freezing' to occur.

5. Conclusion and discussion

Inspired by a recent analysis of ADL kinetics for 1D semi-infinite crystal facets at fixed heights [19], we revisited this system and derived formal expansions for the continuum surface slope in the vicinity of each facet. Our starting point was a system of nonlinear ODEs for discrete slopes according to the BCF model. Each of the steps interacts with its nearest neighbors through elastic-dipole and entropic repulsions. The ODEs were converted to a difference scheme and sum equations via a discrete self-similar solution. In the macroscopic limit, the sum equations are reduced to integral relations which unveil via iterations the local behavior of the continuum slope (and flux) near facets. Our approach is not limited by the kinetics: DL and ADL kinetics in surface diffusion as well as evaporation–condensation are treated formally on the same grounds.

We studied two possible extensions of this approach. First, we considered multipole nearest-neighbor step interactions. For step interactions decaying as $w^{-\alpha}$ with the terrace width w, where $\alpha \geq 2$, the slope vanishes as $\mathcal{O}(\bar{x}^{1/\alpha})$ with the distance $\bar{x}$ from the facet edge, in agreement with notions of local equilibrium. Second, we studied implications of special kinetics at extremal steps, assuming the macroscopic limit is meaningful.

The setting, motivated by [15,19], provides an explicit example of a step flow model consistent with the continuum theory. The conditions of zero slope and flux (e.g., in DL kinetics) are compatible with those afforded by a gradient-flow-type formulation; see, e.g., Odisharia [36], Spohn [12], and Shenoy and Freund [13]. Our work provides a linkage of the underlying particle structure to the local behavior of continuum-scale variables near the facet boundary.

Our approach bears limitations. The self-similar solution studied here is expected to capture the long-time evolution of the slope. The transient near-facet behavior requires a subtler analysis. The derived integral equations have not been studied rigorously; issues of existence and uniqueness of solutions were not touched upon. In the same vein, the legitimacy of applying iterations was not addressed (although an exactly solvable case in evaporation–condensation via self-similarity is pointed out in Appendix C). Self-similar solutions were applied but *not* proved to exist, be unique or stable.

The setting with semi-infinite, 1D and fixed-height facets of this article forms a simplification of (the more realistic) situations where facets are finite, have curved boundaries and time-varying height [7,18]. In such cases, individual steps collapsing on top of the facets can influence the surface profile macroscopically [7]. The derivation of near-facet expansions for the slope in more complicated geometries is the subject of work in progress.

Acknowledgements

Appendix A. Discrete scheme of the evaporation–condensation process

For a specific version of this process, the step velocity law reads [3,12,16]

$$v_j(t) = \frac{\mathrm{d}x_j}{\mathrm{d}t} = \dot{x}_j(t) = -(\mu_j - \mu^0), \quad j = 0, 1, \ldots, N, \tag{A.1}$$

where μ^0 is the chemical potential of the surrounding vapor; set $\mu^0 = 0$. In (A.1), we use a constant mobility; see [23,12,16] for variants of (A.1). In view of (3), we wind up with the discrete scheme

$$\epsilon^{-2}m_j^2(m_{j+1}^3 - 2m_j^3 + m_{j-1}^3) = \dot{m}_j, \quad j = 0, \ldots, N-1, \tag{A.2}$$

along with the termination conditions $m_{-1} = 0 = m_N$.

Heuristically, we can eliminate time via the (particular) self-similar solution

$$m_j(t) = P(t)M_j \qquad (dM_j/dt \equiv 0, \; M_j \neq 0). \tag{A.3}$$

By (A.2), we have $\dot{p}/p^5 = -C = $ const.; set $C = 1$. Thus, $P(t) = (4t + K)^{-1/4}$. The M_j satisfy the *second-order* scheme

$$M_{j+1}^3 - 2M_j^3 + M_{j-1}^3 = -\frac{\epsilon^2}{M_j}, \quad j = 0, \ldots, N-1 \; (M_j > 0), \tag{A.4a}$$

$$M_{-1} = 0 = M_N. \tag{A.4b}$$

Appendix B. On solutions of difference equations

This appendix has details for the computations of Section 3 and Appendix C.

B.1. Second-order difference scheme

First, we indicate how to solve the difference scheme

$$\psi_{j+1} - 2\psi_j + \psi_{j-1} = f_j, \quad j = 0, \ldots, N-1; \\ \psi_{-1} = 0 = \psi_N, \tag{B.1}$$

where f_j are given and can be time dependent. We write

$$\psi_j = \frac{1}{j!} \frac{d^j \Psi(s)}{ds^j}\bigg|_{s=0} = \frac{1}{2\pi i} \oint_\Gamma \frac{\Psi(\zeta)}{\zeta^{j+1}} d\zeta$$

$$(i^2 = -1), \; j = 0, \ldots, N-1, \tag{B.2}$$

by applying the Cauchy integral formula, where Γ is a contour enclosing 0 and $\Psi(s)$ is the generating function (polynomial) defined for complex s by

$$\Psi(s) = \sum_{j=0}^{N-1} \psi_j s^j \quad (s \in \mathbb{C}). \tag{B.3}$$

The goal is to find $\Psi(s)$. Multiplying (B.1) by s^j and summing over j we get

$$s^{-1}[\Psi(s) - \psi_0 + \psi_N s^N] - 2\Psi(s) \\ + s[\Psi(s) + \psi_{-1}s^{-1} - \psi_{N-1}s^{N-1}] = F(s),$$

where

$$F(s) = \sum_{j=0}^{N-1} f_j s^j. \tag{B.4}$$

Thus, we obtain

$$\Psi(s) = \frac{\psi_0 - \psi_{-1}s - \psi_N s^N + \psi_{N-1}s^{N+1} + sF(s)}{(1-s)^2}$$

$$= \frac{\mathcal{P}(s)}{(1-s)^2}. \tag{B.5}$$

The point $s = 1$ is a removable singularity provided $\mathcal{P}(1) = 0 = \mathcal{P}'(1)$.

The coefficient of s^j in $\Psi(s)$ is given by (B.2). By taking the contour Γ in the interior of the unit disk ($|\zeta| < 1$), and eliminating analytic terms, we have

$$\psi_j = \frac{1}{2\pi i} \oint_\Gamma \frac{\psi_0 + \zeta F(\zeta)}{(1-\zeta)^2} \frac{d\zeta}{\zeta^{j+1}}, \quad j = 0, \ldots, N-1. \tag{B.6}$$

Recalling the binomial expansion $(1-\zeta)^{-2} = \sum_{k=0}^\infty (1+k)\zeta^k$, we find the series

$$\frac{\psi_0 + \zeta F(\zeta)}{(1-\zeta)^2} = \psi_0 + \sum_{l=0}^\infty \zeta^{l+1}\left[l + 2 + \sum_{p=0}^l (1+l-p)f_p\right]. \tag{B.7}$$

The coefficient of ζ^j, which by (B.6) yields ψ_j, is singled out for $l = j - 1$.

B.2. Fourth-order difference scheme

Next, consider the difference scheme (22). The generating polynomial, $\Psi(s)$, introduced in (B.3) satisfies

$$s^{-2}(\Psi - \psi_0 - \psi_1 s + \psi_N s^N + \psi_{N+1}s^{N+1}) - 4s^{-1}(\Psi - \psi_0 \\ + \psi_N s^N) + 6\Psi - 4s(\Psi + \psi_{-1}s^{-1} - \psi_{N-1}s^{N-1}) \\ + s^2(\Psi + \psi_{-2}s^{-2} + \psi_{-1}s^{-1} - \psi_{N-1}s^{N-1} - \psi_{N-2}s^{N-2})$$

$$= F(s) = \sum_{j=0}^{N-1} f_j s^j.$$

In view of termination conditions (22b), we find

$$\Psi(s) = \frac{\mathcal{P}(s)}{(1-s)^4}; \tag{B.8a}$$

$$\mathcal{P}(s) = \psi_0 + (\psi_1 - 4\psi_0)s + \psi_0 s^2 + \psi_{N-1}s^{N+1} \\ + (\psi_{N-2} - 4\psi_{N-1})s^{N+2} + \psi_{N-1}s^{N+3} + s^2 F(s). \tag{B.8b}$$

The point $s = 1$ must be a removable singularity in (B.8a); thus, we should have $\mathcal{P}(1) = \mathcal{P}'(1) = \mathcal{P}''(1) = \mathcal{P}'''(1) = 0$, which entails the equations

$$\psi_1 - 2\psi_0 + \psi_{N-2} - 2\psi_{N-1} = -F(1),$$
$$\psi_1 - 2\psi_0 + (N+2)(\psi_{N-2} - 2\psi_{N-1}) = -2F(1) - F'(1),$$
$$2\psi_0 + (N+1)(N+2)\psi_{N-2} - 2(N^2 + 3N + 1)\psi_{N-1} = -2F(1) \\ - 4F'(1) - F''(1),$$
$$N(N+1)(N+2)\psi_{N-2} - 2(N^2 - 1)(N+3)\psi_{N-1} = -6[F'(1) \\ + F''(1)] - F'''(1). \tag{B.9}$$

The solution of this system leads to formulas (25).

We now determine ψ_j in terms of ψ_0 and ψ_1 with recourse to (B.2); Γ is a contour enclosing 0 in the interior of the unit disk. By conveniently removing an analytic part of the integrand, we have (for $j = 0, \ldots, N-1$)

$$\psi_j = \frac{1}{2\pi i} \oint_\Gamma \frac{\psi_0 + (\psi_1 - 4\psi_0)\zeta + \psi_0 \zeta^2 + \zeta^2 F(\zeta)}{(1-\zeta)^4} \frac{d\zeta}{\zeta^{j+1}}. \tag{B.10}$$

By virtue of the binomial expansion

$$(1-\zeta)^{-4} = \frac{1}{3!}\sum_{l=0}^\infty (l+1)(l+2)(l+3)\zeta^l \quad |\zeta| < 1,$$

the integrand in (B.10) has residue at $\zeta = 0$ equal to

$$\frac{1}{3!}\left[\psi_0(j+1)(j+2)(j+3) + (\psi_1 - 4\psi_0)j(j+1)(j+2) \right.$$

$$\left. + \psi_0(j-1)j(j+1) + \sum_{p=0}^{j-2}(j-1-p)(j-p)(j-p+1)f_p\right].$$

By separating distinct powers of j in the first line, we obtain (24).

Appendix C. Continuum limit in evaporation–condensation kinetics

In this appendix, we convert the discrete scheme (A.4) of Appendix A to an integral equation for the continuum-scale, self-similar slope in the limit $\epsilon \downarrow 0$. We also find a near-facet expansion for this slope by direct iterations of the derived integral equation. This iteration procedure is reasonably validated through an exact formula for the (assumed) self-similar continuum solution.

C.1. Integral equation

By $\psi_j = M_j^3$, the relevant difference scheme reads

$$\psi_{j+1} - 2\psi_j + \psi_{j-1} = f_j = -\frac{\epsilon^2}{\psi_j^{1/3}}, \quad \psi_{-1} = 0 = \psi_N, \qquad (C.1)$$

where $\psi_j > 0$ and $j = 0, 1, \ldots, N-1$. We assume $\psi_j \rightharpoonup \psi(h)$ as $\epsilon \downarrow 0$.

Proposition C.1 (*A Continuum Limit in Evaporation–Condensation*)*.* In the limit $\epsilon \downarrow 0$, discrete scheme (C.1) reduces to the integral equation

$$\psi(h) = m(h)^3 = C_1 h - \int_0^h \frac{h-z}{m(z)} dz \quad 0 < h < 1; \qquad (C.2)$$

thus, $\lim_{h\downarrow 0} m(h) = 0$. The constant C_1 is

$$C_1 = \int_0^1 \frac{1-z}{\psi(z)^{1/3}} dz = \int_0^1 \frac{1-z}{m(z)} dz > 0, \qquad (C.3)$$

which implies $\lim_{h\uparrow 1} m(h) = 0$. By (C.2), a sufficiently differentiable $m(h)$ satisfies the ODE $m(m^3)_{hh} = -1$ for $0 < h < 1$.

By abusing notation, we use the symbol $m(h)$ for the space-dependent part of the self-similar slope; i.e., $m(h, t) = P(t)m(h) = (4t + K)^{-1/4}m(h)$. Assume that the integral in (C.2) converges and a solution exists appropriately.

Proof. Starting with (C.1) and finite N, we express ψ_j in terms of a (finite) sum over f_j by following the procedure of Appendix B.1. The associated generating polynomial, $\Psi(s)$, introduced in (B.3) is found to be

$$\Psi(s) = \frac{\psi_0 + \psi_{N-1}s^{N+1} + sF(s)}{(1-s)^2}, \quad F(s) = \sum_{j=0}^{N-1} f_j s^j, \qquad (C.4)$$

where ψ_0 and ψ_{N-1} are such that $s = 1$ is a removable singularity of $\Psi(s)$:

$$\psi_0 = \frac{-NF(1) + F'(1)}{N+1}, \qquad \psi_{N-1} = -\frac{F(1) + F'(1)}{N+1}. \qquad (C.5)$$

The prime denotes the derivative of $F(s)$. By (B.2) of Appendix B.1, we find

$$\psi_j = (1+j)\psi_0 + \sum_{p=0}^{j-1}(j-p)f_p = (1+j)\psi_0$$

$$- \sum_{p=0}^{j-1}\epsilon[(j+1)\epsilon - (p+1)\epsilon]\psi_p^{-1/3}. \qquad (C.6)$$

This is the desired sum equation for ψ_j.

Let us now focus on the limit of (C.6) as $\epsilon \downarrow 0$ with $(j+1)\epsilon = h = \mathcal{O}(1)$. With regard to the computation of ψ_0 by (C.5), note that

$$(N+1)\psi_0 = \sum_{j=0}^{N-1}[(N+1)\epsilon - (j+1)\epsilon]\psi_j^{-1/3}\epsilon$$

$$\xrightarrow[\epsilon\downarrow 0]{} \int_0^1 (1-h)\psi(h)^{-1/3}dh, \qquad (C.7)$$

assuming that the respective sum and integral are convergent; thus,

$$\lim_{\epsilon\downarrow 0}(\epsilon^{-1}\psi_0) =: C_1 = \int_0^1 \frac{1-h}{\psi(h)^{1/3}}dh = \int_0^1 \frac{1-h}{m(h)}dh. \qquad (C.8)$$

Let $z = (p+1)\epsilon$ in (C.6); then, by $\psi_p \rightharpoonup \psi(z)$, we have

$$\sum_{p=0}^{j-1}[(j+1)\epsilon - (p+1)\epsilon]\psi_p^{-1/3}\epsilon \rightharpoonup \int_0^h (h-z)\psi(z)^{-1/3}dz. \qquad (C.9)$$

In view of (C.8), we wind up with (C.2) and (C.3). The ODE $m(m^3)_{hh} = -1$ ensues by differentiation (in the usual calculus sense) of the integral equation. This assertion concludes our formal derivation. $\square$

C.2. Iteration scheme and near-facet expansion

Proposition C.1 suggests what the behavior of m near facet edges should be. The integral in (C.2) produces a subdominant contribution $\mathcal{O}(h^{2-\alpha})$ if $m(h) = \mathcal{O}(h^\alpha)$ as $h \downarrow 0$ for some $0 \leqslant \alpha < 1$. A formal expansion can be derived as follows. Set $m(h) \sim m^{(n)}(h)$ to $n + 1$ terms as $h \downarrow 0$, where

$$m^{(n+1)}(h)^3 = C_1 h - \int_0^h \frac{h-z}{m^{(n)}(z)}dz; \qquad m^{(0)}(h) = (C_1 h)^{1/3}. (C.10)$$

Consider $\{m^{(n)}(h)\}_{n=0}^\infty$, defined recursively by (C.10). We compute

$$n = 1: \quad m^{(1)}(h) = \left(C_1 h - \frac{9}{10}C_1^{-1/3}h^{5/3}\right)^{1/3}$$

$$\Rightarrow m^{(1)}(h) - m^{(0)}(h) = -\frac{3}{10}C_1^{-1}h + \mathcal{O}(h^{5/3}) \quad \text{as } h \downarrow 0. \quad (C.11)$$

More generally, the difference $\delta m^{(n)} = m^{(n)} - m^{(n-1)}$ satisfies

$$\delta m^{(n)}[m^{(n)2} + m^{(n)}m^{(n-1)} + m^{(n-1)2}](h)$$

$$= \int_0^h \frac{(h-z)\delta m^{(n-1)}(z)}{m^{(n-1)}(z)m^{(n-2)}(z)}dz \qquad (C.12)$$

for $n = 2, \ldots; m^{(n)}(h) \sim (C_1 h)^{1/3}$ for every n as $h \downarrow 0$. By inspection of (C.11) and (C.12), we see that $\delta m^{(n)}(h) \sim a_n h^{b_n}$. For instance, for $n = 2$ we compute $a_2 = -(9/280)C_1^{-7/3}$, $b_2 = 5/3$ and

$$m^{(2)} \sim m^{(1)}(h) - \frac{9}{280}C_1^{-7/3}h^{5/3}$$

$$= \left(C_1 h - \frac{9}{10}C_1^{-1/3}h^{5/3}\right)^{1/3} - \frac{9}{280}C_1^{-7/3}h^{5/3},$$

which leads to a three-term expansion for $m(h)$:

$$m(h) = (C_1 h)^{1/3} - \frac{3}{10}C_1^{-1}h - \frac{171}{1400}C_1^{-7/3}h^{5/3} + \mathcal{O}(h^{7/3})$$

$$\text{as } h \downarrow 0. \qquad (C.13)$$

Higher-order terms are generated in an analogous fashion, but of course the algebra becomes increasingly cumbersome with the order, n. Our construction implies $m^{(n+1)} - m^{(n)} = \mathcal{O}(h^{(2n/3)+1})$. In Appendix C.3, we show that (C.13) is consistent with the exact, global self-similar solution of the PDE.

The above formal expansion can be converted to a power series in $x - x_{f,L}$, where $x_{f,L}(t)$ is the position of the left facet edge. By $\dot{x}_j = -\mu_j = -\epsilon^{-1}(m_j^3 - m_{j-1}^3)$, and the ansatz $m_j(t) = (4t + K)^{-1/4}M_j$, we ascertain that $x_j(t) \sim t^{1/4}X_j$ for large t. Hence, the similarity coordinate is $\eta = xt^{-1/4}$ and we set $h = h(\eta)$; $m(h(\eta)) = h'(\eta)$. By integrating (C.13), we obtain

$$C_1^{1/3}(\eta - \eta_{f,L}) = \frac{3}{2}h^{2/3} + \frac{9}{40}C_1^{-4/3}h^{4/3}$$

$$+ \frac{1305}{2800}C_1^{-8/3}h^2 + \mathcal{O}(h^{8/3}) \quad \text{as } h \downarrow 0,$$

where $\eta_{f,L} = x_{f,L}(t)t^{-1/4}$. By inverting in the limit $\bar{\eta} = \eta - \eta_{f,L} \downarrow 0$, we find

$$m(h(\eta)) = \left(\frac{2}{3}\right)^{3/2} C_1^{1/2} \left[\frac{3}{2}\bar{\eta}^{1/2} - \frac{3}{8}C_1^{-1}\bar{\eta}^{3/2}\right.$$
$$\left. - \frac{971}{1600}C_1^{-2}\bar{\eta}^{5/2} + \mathcal{O}(\bar{\eta}^{7/2})\right]. \quad (C.14)$$

For the other end point ($h \uparrow 1$), mirror symmetry applies (under $h \mapsto 1 - h$).

Remark C.1. Integral equation (C.2) can result from integrating the ODE $(m^3)_{hh} = -1/m$ via imposing from the outset $m \to 0$ as $h \downarrow 0$ and $h \uparrow 1$. Here, this zero-slope condition emerges directly from the discrete scheme.

Remark C.2. It is tempting to extend the above calculation to the full time-dependent setting, with focus on ODEs (A.2). Consider $m_j(t) \rightharpoonup m(h, t)$. Formally, $1/m(h)$ (under self-similarity) is now replaced by $\partial_t[m(h, t)^{-1}]$ in defining f_j. If the integral converges, the relation for $m(h, t)$ now reads

$$m(h, t)^3 = C_1(t)h - \int_0^h (h - z)\partial_t[m(z, t)^{-1}]dz \quad t > 0; \quad (C.15)$$

$C_1(t)$ is given by the t-dependent counterpart of (C.3). Alternatively, differentiate to get the PDE $\partial_t m = m^2 \partial_h^2(m^3)$ [16]. Caution should be exercised though: in principle, (C.15) may not be amenable to iterations in the sense described above, unless t is sufficiently large. Hence, it is not advisable to iterate (C.15) to study transients of the slope near the facet edge.

Remark C.3. This discussion suggests that, for a class of initial data,

$$m(h(x, t), t) = \mathcal{O}((x - x_f(t))^{1/2}) \quad x \to x_f(t), \quad (C.16)$$

at the left- or right-facet edge position, $x_f(t)$, for sufficiently long times. This behavior is in agreement with the condition of local equilibrium at facet edges [30,32]. The integral equation formulation indicates the *form* of the expansion for $m(h, t)$ and readily provides the leading-order term. For the derivation of higher-order terms, one may use the respective PDE. The starting point is the power series expansion $\sum_{n=1}^{\infty} A_n(x - x_f(t))^{n/2}$, indicated by iterations of (C.2).

C.3. Exact, global self-similar solution

It is rather fortuitous that $m(h)$ can be determined globally [37], thus rendering possible a comparison with expansion (C.13). By $\psi(h) = m(h)^3$, the governing ODE is $\psi'' = -\psi^{-1/3}$, where the prime denotes the derivative in h. If $\psi(0) = 0 = \psi(1)$, by symmetry we can restrict $\psi(h)$ in $(0, 1/2)$ where $\psi'(h) \geqslant 0$ and $\psi'(1/2) = 0$. The ODE is split into the system

$$\psi' = w, \qquad w' = -\psi^{-1/3}, \quad (C.17)$$

to which we associate a constant of motion via the "energy"

$$\mathcal{E}(h) = \frac{1}{2}w(h)^2 + \frac{3}{2}\psi(h)^{2/3}; \qquad \mathcal{E}'(h) = 0. \quad (C.18)$$

Thus, solutions of (C.17) can be parametrized by the constant $c = \mathcal{E}(h)$.

Suppose that we look for solutions consistent with integral equation (C.2). So, we require that ψ and w solve (C.17) for $h \in (0, 1/2)$ under the conditions

$$\psi(0) = 0, \qquad w(1/2) = 0. \quad (C.19)$$

By definition of $\mathcal{E}$ and w we compute $h(m)$ in closed form by

$$h = \int_0^\psi \frac{d\xi}{\sqrt{2c - 3\xi^{2/3}}} = \frac{c}{\sqrt{3}}\left(\sin^{-1}\widetilde{m} - \widetilde{m}\sqrt{1 - \widetilde{m}^2}\right);$$
$$\widetilde{m} = m\sqrt{\frac{3}{2c}} \quad (C.20)$$

and $0 \leq h \leq 1/2$ along with $w = d\psi/dh \geqslant 0$. The solution $h(m)$ for $1/2 < h \leq 1$ is obtained by reflection. In principle, (C.20) (and its reflection) can be inverted to generate $m(h)$. The constant c can be found by setting $h = 1/2$ in (C.20) and using the definition of $\mathcal{E}(h)$ and $w(1/2) = 0$. Thus, we deduce

$$\frac{1}{2} = \int_0^{\psi(1/2)} \frac{d\xi}{\sqrt{2c - 3\xi^{2/3}}}, \quad (C.21)$$
$$c = 3\psi(1/2)^{2/3}/2 \Rightarrow c = \sqrt{3}/\pi,$$

and $m(1/2) = 3^{-1/4}2^{1/2}\pi^{-1/2}$.

We proceed to generate a power series of $m(h)$. Eq. (C.20) becomes

$$\pi h = \sum_{l=1}^{\infty} \frac{\Gamma\left(\frac{1}{2} + l\right)}{l!\Gamma\left(\frac{1}{2}\right)} \frac{4l}{4l^2 - 1}\widetilde{m}^{2l+1} \quad \widetilde{m} < 1,$$

where $\Gamma(z)$ is the Gamma function. The inversion of the last series yields

$$\widetilde{m}(h)^3 = \frac{3\pi h}{2} - \frac{3}{10}\left(\frac{3\pi h}{2}\right)^{5/3} - \frac{3}{280}\left(\frac{3\pi h}{2}\right)^{7/3} + \mathcal{O}(h^3)$$
$$\text{as } h \downarrow 0. \quad (C.22)$$

This expansion is consistent with (C.13) by $C_1 = 3^{1/4}2^{1/2}\pi^{-1/2}$. The full h-expansion, by inversion of (C.20), is convergent in a vicinity of $h = 0$.

Appendix D. Iteration of the integral equation for DL kinetics

In this appendix, we discuss the use of iterations for formally constructing an expansion of the continuum-scale slope near facet edges in the DL case (Section 3.1). Consider scheme (18). Because of the increasingly elaborate algebra, we compute up to three terms for $m(h(\eta))$.

$$m^{(1)}(h)^3 = C_1 h - \int_0^h \frac{h - z}{(C_1 z)^{1/3}}C_2 z dz = C_1 h - \frac{9}{40}\frac{C_2}{C_1^{1/3}}h^{8/3}, \quad (D.1)$$

$$\varphi^{(1)}(h) = C_2 h - \int_0^h \frac{h - z}{(C_1 z)^{1/3}}dz = C_2 h - \frac{9}{10}C_1^{-1/3}h^{5/3};$$

$$\Rightarrow \frac{\varphi^{(1)}(h)}{m^{(1)}(h)} = \frac{C_2}{C_1^{1/3}}h^{2/3} - \frac{9}{10}C_1^{-2/3}h^{4/3} + \mathcal{O}(h^{7/3}) \quad h \downarrow 0.$$

Accordingly, an approximation for $m^{(2)}(h)$ comes from

$$m^{(2)}(h)^3 = C_1 h - \int_0^h (h - z)\frac{\varphi^{(1)}(z)}{m^{(1)}(z)}$$
$$= C_1 h - \frac{9}{40}\frac{C_2}{C_1^{1/3}}h^{8/3} + \frac{3^4}{700}C_1^{-2/3}h^{10/3} + \mathcal{O}(h^{13/3}), \quad (D.2)$$

which leads to (19), where $m(h(\eta)) = h'(\eta)$. By integrating in η we find

$$\bar{\eta} = \frac{3}{2}C_1^{-1/3}h^{2/3} + \frac{9}{280}\frac{C_2}{C_1^{5/3}}h^{7/3} - \frac{9}{700}C_1^{-2}h^3 + \mathcal{O}(h^4) \quad h \downarrow 0.$$

The inversion of this expansion yields

$$h(\eta) = \left(\frac{2}{3}\right)^{3/2} C_1^{1/2}\bar{\eta}^{3/2} - \frac{2}{315}C_2\bar{\eta}^4 + \frac{8}{4725}\bar{\eta}^5 + \mathcal{O}(\bar{\eta}^{13/2}), \quad (D.3)$$

which is reduced to (20) through differentiation.

References

[1] M. Pulvirenti, Kinetic limits for stochastic particle systems, in: D. Talay, L. Tubaro (Eds.), in: Lecture Notes in Mathematics, vol. 1627, Springer, Berlin, 1996, pp. 96–126.

[2] H. Spohn, Large Scale Dynamics of Interacting Particles, Springer, Berlin, 1991.

[3] H.-C. Jeong, E.D. Williams, Steps on surfaces: experiments and theory, Surf. Sci. Rep. 34 (1999) 171–294.

[4] P. Nozières, On the motion of steps on a vicinal surface, J. Phys. France 48 (1987) 1605–1608.

[5] A. Rettori, J. Villain, Flattening of grooves on a crystal surface: a method of investigation of surface roughness, J. Phys. France 49 (1988) 257–267.

[6] M. Ozdemir, A. Zangwill, Morphological equilibration of a corrugated crystalline surface, Phys. Rev. B 42 (1990) 5013–5024.

[7] N. Israeli, D. Kandel, Profile of a decaying crystalline cone, Phys. Rev. B 60 (1999) 5946–5962.

[8] W. E, N.K. Yip, Continuum theory of epitaxial growth. I, J. Stat. Phys. 104 (2001) 221–253.

[9] R.V. Kohn, T.S. Lo, N.K. Yip, Continuum limit of a step flow model of epitaxial growth, in: M.C. Bartelt, J.W. Evans, A.S. Karma, S. Torquato, D.E. Wolf (Eds.), Statistical Mechanical Modeling in Materials Science, MRS Symposia Proceedings No. 701, Materials Research Society, Warrendale, PA, 2002, pp. T1.7.1–T1.7.7.

[10] Y. Xiang, Derivation of a continuum model for epitaxial growth with elasticity on vicinal surface, SIAM J. Appl. Math. 63 (2002) 241–258.

[11] D. Margetis, R.V. Kohn, Continuum relaxation of interacting steps on crystal surfaces in 2 + 1 dimensions, Multiscale Model. Simul. 5 (2006) 729–758.

[12] H. Spohn, Surface dynamics below the roughening transition, J. Phys. I France 3 (1993) 69–81.

[13] V.B. Shenoy, L.B. Freund, A continuum description of the energetics and evolution of stepped surfaces in strained nanostructures, J. Mech. Phys. Solids 50 (2002) 1817–1841.

[14] D. Margetis, M.J. Aziz, H.A. Stone, Continuum approach to self-similarity and scaling in morphological relaxation of a crystal with a facet, Phys. Rev. B 71 (2005) 165432.

[15] P.-W. Fok, R.R. Rosales, D. Margetis, Facet evolution on supported nanostructures: the effect of finite height, Phys. Rev. B 78 (2008) 235401.

[16] H.A. Stone, M.J. Aziz, D. Margetis, Grooving of a grain boundary by evaporation–condensation below the roughening transition, J. Appl. Phys. 97 (2005) 113535.

[17] A. Chame, S. Rousset, H.P. Bonzel, J. Villain, Slow dynamics of stepped surfaces, Bulg. Chem. Commun. 29 (1996–1997) 398–434.

[18] D. Margetis, P.-W. Fok, M.J. Aziz, H.A. Stone, Continuum theory of nanostructure decay via a microscale condition, Phys. Rev. Lett. 97 (2006) 096102.

[19] H. Al Hajj Shehadeh, R.V. Kohn, J. Weare, The evolution of a crystal surface: analysis of a 1D step train connecting two facets in the ADL regime, preprint.

[20] D.T.J. Hurle (Ed.), Handbook of Crystal Growth, North Holland, Amsterdam, 1993.

[21] T. Michely, J. Krug, Islands, Mounds and Atoms: Patterns and Processes in Crystal Growth Far from Equilibrium, Springer, Berlin, 2004.

[22] O. Pierre-Louis, Dynamics of crystal steps, C. R. Phys. 6 (2005) 11–21.

[23] A. Pimpinelli, J. Villain, Physics of Crystal Growth, Cambridge, UK, 1998.

[24] W.K. Burton, N. Cabrera, F.C. Frank, The growth of crystals and the equilibrium structure of their surfaces, Philos. Trans. R. Soc. Lond. Ser. A 243 (1951) 299–358.

[25] V.I. Marchenko, A.Ya. Parshin, Elastic properties of crystal surfaces, Sov. Phys. JETP 52 (1980) 129–131.

[26] R. Najafabadi, J.R. Srolovitz, Elastic step interactions on vicinal surfaces of fcc metals, Surf. Sci. 317 (1994) 221–234.

[27] N. Israeli, H.-C. Jeong, D. Kandel, J.D. Weeks, Dynamics and scaling of one-dimensional surface structures, Phys. Rev. B 61 (2000) 5698–5706.

[28] P.-W. Fok, R.R. Rosales, D. Margetis, Unification of step bunching phenomena on vicinal surfaces, Phys. Rev. B 76 (2007) 033408.

[29] N. Israeli, D. Kandel, Decay of one-dimensional surface modulations, Phys. Rev. B 62 (2000) 13707–13717.

[30] H.P. Bonzel, 3D equilibrium crystal shapes in the new light of STM and AFM, Phys. Rep. 385 (2003) 1–67.

[31] E.E. Gruber, W.W. Mullins, On the theory of anisotropy of crystalline surface tension, J. Phys. Chem. Solids 28 (1967) 875–887.

[32] C. Jayaprakash, W.F. Saam, S. Teitel, Roughening and facet formation in crystals, Phys. Rev. Lett. 50 (1983) 2017–2020.

[33] D. Margetis, A.E. Tzavaras, Kinetic hierarchies and macroscopic limits for crystalline steps in 1 + 1 dimensions, Multiscale Model. Simul. 7 (2009) 1428–1454.

[34] G. Ehrlich, F. Hudda, Atomic view of surface diffusion: tungsten on tungsten, J. Chem. Phys. 44 (1966) 1039–1099.

[35] R.L. Schwoebel, E.J. Shipsey, Step motion on crystal surfaces, J. Appl. Phys. 37 (1966) 3682–3686.

[36] I.V. Odisharia, Simulation and analysis of the relaxation of a crystalline surface, Ph.D. Thesis, New York University, 2006.

[37] M.G. Grillakis, Private communication, 2010.